

Lasers in Manufacturing Conference 2021

# Ultrashort pulse laser cutting of clear polyimide and hard coat film stacks for flexible OLED displays

Jim Bovatsek<sup>a,\*</sup>

<sup>a</sup>MKS Spectra-Physics, 1565 Barber Lane, Milpitas, CA 95035-7409, United States

---

## Abstract

New mobile devices include flexible and foldable OLED displays which require new protective cover materials. Options for this include ultrathin glass (UTG) as well as a new type of clear polyimide (clear PI), which is transparent at visible wavelengths. The clear PI is combined with a scratch resistant hard coat (HC) layer and a final PET (polyethylene terephthalate) protective film. Here we present results for cutting thick clear PI/HC/PET layered stacks using high power UV ultrashort pulse lasers. Ablation thresholds were found to vary by almost a factor of ten, and a layer-optimized cutting approach was used. The optimized cutting process is of high quality and throughput, with heat-affect zone (HAZ) of <10  $\mu\text{m}$  and cutting speed of >400 mm/s. These results are comparable to that for individual sheets of polymers used in OLED display manufacturing.

Keywords: OLED display; foldable phone; polymer film; picosecond UV laser; ablation threshold

---

## 1. Main text

The touch panel display is one of the most important components in today's advanced mobile devices. While processing power and wireless data technology are clearly important differentiators, the display itself serves as the primary human interface component and therefore plays a critical role in shaping the user's experience. In recent years, OLED (organic light-emitting diode) displays have risen to prominence in the mobile device market. They offer excellent image quality in a thin, flexible, lightweight and energy efficient package, which make them ideal for current and future generations of foldable mobile devices.

---

\* Corresponding author.

E-mail address: Jim.Bovatsek@mksinst.com .

The key challenge of a compact foldable phone is achieving a small bending radius of curvature in components within the display (OLED panel, touch sensor, polarizer, cover window). For this purpose, manufacturers continue to develop materials such as ultrathin glass (UTG) and a relatively new type of polyimide—clear polyimide (clear PI)—that is highly transparent at visible wavelengths. While UTG is inherently more scratch resistant, it is also brittle and challenging to both manufacture and handle at the required thicknesses (<50-200  $\mu\text{m}$ ). Clear PI is inherently flexible and has manufacturability advantages, but it must be covered with a thin hard coat (HC) layer to improve its scratch resistance. This coating can also be engineered for anti-glare and anti-fingerprint properties. Both materials are expected to have a strong presence going forward in the foldable display market. For UTG glass cutting, Bessel beam processing with an IR picosecond laser is a known viable option; for clear PI + HC, ablation cutting is required.

In this work, we present results using a high power picosecond 355 nm hybrid fiber laser (Spectra-Physics® IceFyre® 355-50) for ablation cutting of a clear PI-based multi-layer stack for foldable display cover window application. The stack is comprised of a 50  $\mu\text{m}$  thick clear PI film with a 12  $\mu\text{m}$  thick HC layer on one surface. Adhered to the HC layer is a protective layer (to be removed later) of 50  $\mu\text{m}$  thick polyethylene terephthalate (PET). Additionally, the PET film has a pressure sensitive adhesive (PSA) coating ( $\sim 4 \mu\text{m}$ ) for adherence to the hard coated surface of the clear PI. While high quality is imperative for the clear PI+HC layers, it is important but not as critical for the PET + PSA film.

### 1.1. Experimental Details

The basic parameters for the laser source used in this work are detailed in Table 1. All processing was performed with a high speed and precision 2-axis scanning galvanometer coupled with an F=163 mm telecentric f-theta focusing objective. No beam expansion was used, and the focused beam diameter created by the system was  $\sim 16\text{-}18 \mu\text{m}$ ,  $1/e^2$  (calculated and confirmed experimentally).

Table 1. Parameters listing for laser used in the experiments

| IceFyre 355-50 laser    | Value       | Units         |
|-------------------------|-------------|---------------|
| Average power           | >50         | W             |
| Max. pulse energy       | >40         | $\mu\text{J}$ |
| Nominal pulse frequency | 1.25        | MHz           |
| Pulse duration, typical | 10          | ps            |
| Beam diameter           | 5.0 +/- 0.5 | mm            |

### 1.2. Materials

The material tested is a layered polymer stack developed by a materials supplier to the OLED display manufacturing industry. While it has several potential uses, that of a protective cover window for foldable phones is a key motivation. A cross-section diagram of the multilayer stack is shown below (Fig. 1).

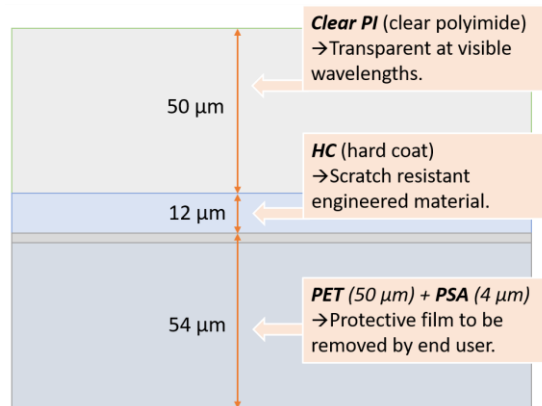


Fig. 1. Cross-section reference diagram showing the clear PI, hard coat, and PET protective layer for foldable OLED protective cover window.

The 12 μm thick hard coat film is an advanced engineered coating, typically an organic polymerized film with embedded inorganic particles such as high-hardness glass/ceramic nanoparticles. It may be designed for a range of engineered properties, including anti-fingerprint and anti-glare in addition to scratch resistance. The substrate for this film, clear PI, has the high mechanical strength and temperature handling of conventional polyimide, but has high transparency across the visible wavelength spectrum and hence lacks any shaded tint (such as orange/yellow of conventional PI). The PET (with thin pressure-sensitive adhesive (PSA)) film is for protection throughout the processing of the entire display and is ultimately removed by the end user. Hence, while quality is important for cutting the PET, it is not critical. The most critical quality demand is on the HC layer, which provides the exterior interface surface not only for customer use but also potentially for mounting/confining the display itself.

## 2. Results

Experimental results are comprised of two main sections: ablation thresholds and full stack cutting. For thresholds testing, the Liu method (Ref. 1) was used to determine ablation thresholds for single pulse irradiation. For full cutting results, the thresholds data previously determined, as well as observations made during the tests, were considered for the development of a process to fully cut through the material. This full cutting was achieved by combining three layer-specific processes, each optimized to deliver best speed and quality for the respective material.

### 2.1. Ablation thresholds

Implementing the Liu threshold method, which uses linear regression analysis of the ablated area relative to the pulse energy used, single-pulse ablation thresholds were determined independently for the clear PI, HC, and PET layers. Pre-screening was used to determine the range of pulse energies most suitable for generating useful data for the tests. If the pulse energy is too high relative to the (as yet unknown) threshold, the ablation craters typically have non-uniformities and deviations from the expected Gaussian beam-defined shape, resulting in poorly correlated thresholds data. A data plot showing the thresholds data (ablation area vs.

fluence) for the clear PI, HC, and PET layers is shown in Fig. 2. Also included are markers highlighting the thresholds (in  $\text{J}/\text{cm}^2$ ) of each material.

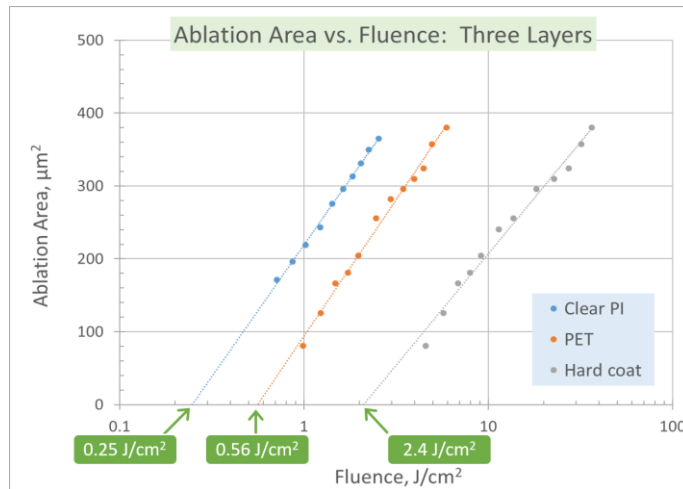


Fig. 2. Single-pulse ablation thresholds and data for clear PI, hard coat, and PET materials.

The data shows that the thresholds vary considerably amongst the three constituent materials. The clear PI is quite low at  $\sim 0.25 \text{ J}/\text{cm}^2$ , which indicates a similar response to the UV wavelength as with conventional polyimide (i.e. strong linear absorption). The PET material has a threshold more than 2× higher at  $\sim 0.56 \text{ J}/\text{cm}^2$ , which likely signifies the relatively high transparency at 355 nm. Lastly, the HC material is shown to have a very high threshold, at nearly 10× higher than that for its clear PI substrate. This threshold value ( $\sim 2.4 \text{ J}/\text{cm}^2$ ) is in the range of what is typically expected for various glass materials with ultrashort pulse lasers.

For qualitative analysis, optical microscope images of ablation craters for each material were generated (Fig. 3). The highlighted features correspond to ablation using energy densities of approximately 5× each material's threshold fluence. As with the thresholds, we see significant variation across the materials.

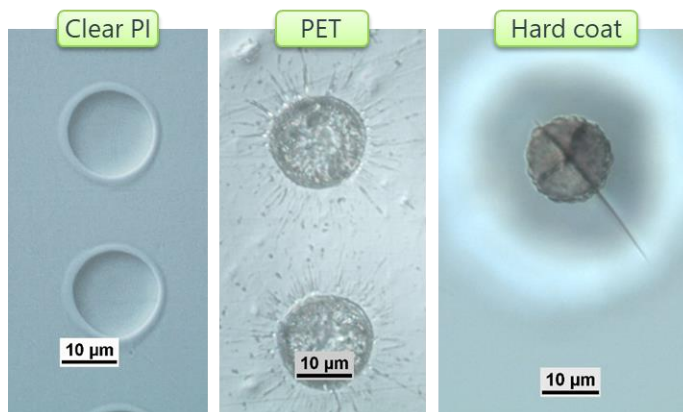


Fig. 3. Optical microscope images of single-pulse ablation craters in clear PI, hard coat, and PET materials.

The clear PI shows very clean ablation as might be anticipated based on its low threshold. The lack of debris and smooth, shallow craters are indicative of the kind of high-quality photoablation known to occur at the UV wavelength, even with ns pulse widths. The PET ablation craters by contrast exhibit a much poorer appearance. The irregularity of the crater floor is likely related to the weak linear optical absorption while the radial “splatter” artifacts reflect the relatively low melting temperature. Lastly, the HC material shows yet another variation in appearance. While the edge boundary and crater floor are relatively well-defined and free of melt and debris, there is noticeable microcracking. In the aggregate, the highly variable thresholds data combined with the ablation crater qualitative differences present a significant challenge for developing a full stack cutting process.

## *2.2. Full Stack Cutting*

The results from the threshold study clearly show there are various challenges for developing a full stack cutting process. Typically, laser process optimization hinges on two key aspects—throughput and quality. From the clear PI ablation results, quality is obviously not an issue due to strong optical absorption and corresponding UV photoablation. At the same time, however, the strong (shallow) absorption means per-pulse ablation rates are somewhat limited. Moreover, with such a low ablation threshold, there are challenges related to translating the laser’s high average power and pulse energy into a high cutting speed. Therefore, the clear PI presents a throughput challenge. It is evident that the HC layer, on the other hand, presents a quality challenge, given its apparent brittleness and tendency to crack with just a single irradiating pulse.

### *2.2.1. Throughput optimization: clear polyimide*

Given the presumed high transparency of the HC film and the strong absorption of the clear PI, it was concluded that a full cutting process should begin with the clear PI surface and continue down through the subsequent layers. If the cutting was attempted first through the transparent PET and HC layers, the strong absorption at the clear PI interface would likely promote heating and layer delamination (this expected issue was in fact confirmed experimentally). Therefore, the problem existed of quickly cutting through the clear PI but also creating a relatively wide kerf width to allow a maximum amount of light through to the significantly higher threshold HC layer.

With this goal, a series of tests was performed aimed at maximizing both the ablation kerf width and depth in the clear PI. This was done by varying the amount of optical system defocusing (0-2.5 mm with 0.5 mm increments) and laser pulse repetition frequency PRF (1.25, 1.50, 1.75, 2.0 MHz). Scribes at each condition were generated using 10 repeated, overlaying scans at a scan speed of 10 m/s (10/10 = 1 m/s net scribing speed). The corresponding laser average powers for the four PRF settings were 50, 46, 42, and 38 W (low → high PRF). The results of the defocusing tests are displayed in Fig. 4 below.

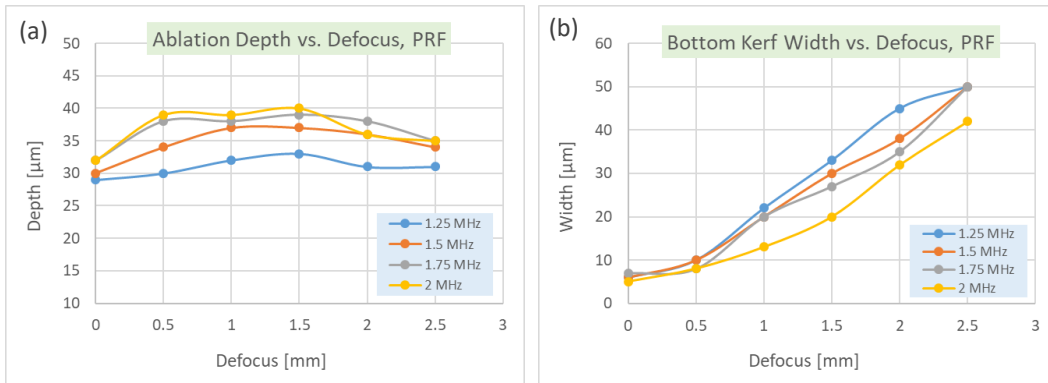


Fig. 4. (a) shows scribe depth vs. defocus and PRF; (b) shows bottom kerf width vs. defocus and PRF.

From Fig. 4(a), the lowest repetition rate of 1.25 MHz offers a distinctly shallow scribing depth compared to the others, and a defocus of 1.5 mm yields the deepest trenches overall. With 1.5 mm of defocus from the beam waist, the calculated  $1/e^2$  Gaussian spot size is  $\sim 42 \mu\text{m}$ . From Fig. 4(b), the highest PRF of 2 MHz is the clear outlier, generating the narrowest kerf width throughout the range of focus positions. With this data for kerf depth and width, a laser PRF of 1.65 MHz and a defocus position of 1.25 mm were chosen for the clear PI full cutting process.

### 2.2.2. Quality optimization: hard coat film

From the thresholds data, it was clear that achieving a high quality scribe/cut in the HC would be a challenge. Given that microcracking was observed with just a single pulse, a conventional approach of low-moderate fluence and pulse overlap process would not likely succeed. This was demonstrated experimentally, with scribe at 65% pulse overlap yielded severe chipping. On the other hand, it was discovered that a significantly high pulse overlap process of  $\sim 94\%$  yielded exceptional quality of scribes in the HC film. A collection of microscope photos showing single pulse ablation crater in HC alongside scribes generated with low and high pulse overlap processes is shown in Fig. 5.

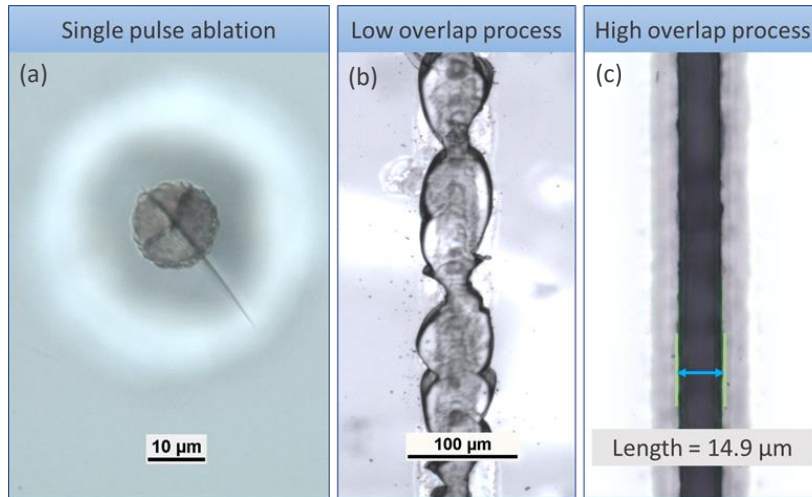


Fig. 5. (a) single pulse ablation in HC showing microcracks; (b) low overlap (67%) process with severe edge chipping; (c) very high overlap (94%) process demonstrating very good edge quality.

A key difference between this HC scribe test and what is needed for a full stack cutting process is that the light is incident from different directions. Fig. 5 shows the results with the beam incident directly on the HC surface whereas for a full cutting process the beam first cuts through the clear PI before meeting the HC layer. However, the data generated in this test were used to guide the parameter selection for the layer-specific full stack cutting process development.

### 2.2.3. Full stack cutting process

With the throughput and quality challenges addressed for the most critical layers of the stack, parameters were then optimized for cutting the full stack. After process fine-tuning, very exceptional quality results were achieved. Three layer-specific process were combined and executed sequentially, encompassing a range of laser PRFs from 1.65 – 3 MHz, laser average powers from 28 – 45 W, and scanning speeds from 3 – 10 m/s with a total of 20 overlapping scans. Factoring in the number of scans required at each respective scan speed, the overall (net) cutting speed for the process was >400 mm/s. Microscope images in Fig. 6 below demonstrate the excellent edge quality of the cuts for each material.

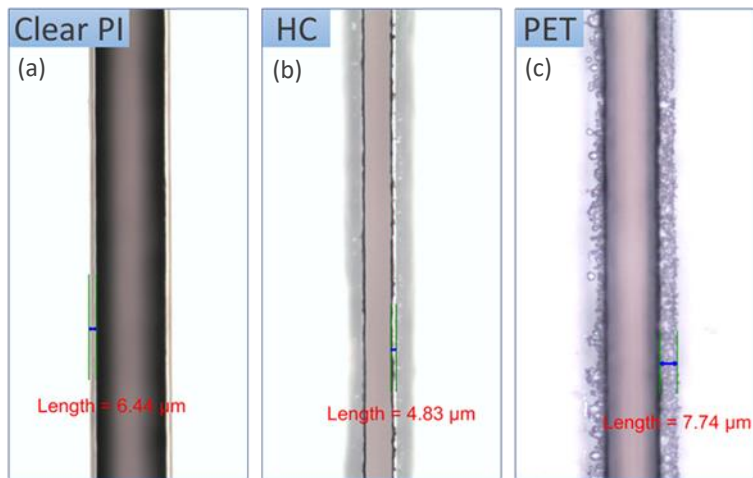


Fig. 6. (a) microscope photo showing 6-7  $\mu\text{m}$  edge heat affected zone (HAZ) in clear PI; (b) laser-cut HC layer with  $<5 \mu\text{m}$  edge chipping; (c) debris and HAZ confined to  $<8 \mu\text{m}$  in the PET protective film.

For all materials, edge effects such as HAZ, chipping, debris, etc., are well below  $10 \mu\text{m}$ , with less than  $5 \mu\text{m}$  achieved for the most challenging HC film. For OLED polymer cutting, HAZ below  $20 \mu\text{m}$  is generally acceptable. It is interesting and noteworthy that, although the HC cutting process was largely optimized with the laser incident onto its outward surface, the same exceptional quality is achieved with only minor process tuning when first cutting through the clear PI layer. Finally, for the less critical PET film, the edge quality is still very good, with molten recast limited to  $<10 \mu\text{m}$ . A cross-section inspection was also performed, with microscope photo shown in Fig. 7.

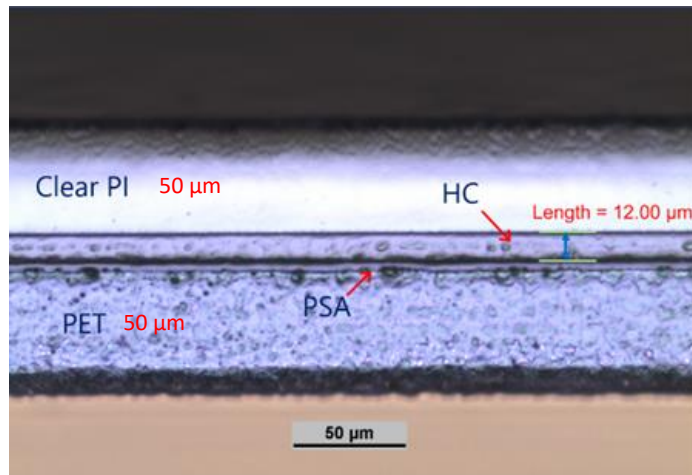


Fig. 7. Microscope photo showing cross-section of laser-cut film stack; no layer delamination or debris “smearing” across the cut surfaces is evident.



The cross-section image in Fig. 7 shows that high cutting quality is maintained throughout the full thickness of the stack. There is no evidence of layer delamination which might be expected for such a combination of materials having a diverse range of optical, thermal, and mechanical properties. Furthermore, the presence of even a thin PSA layer can often be troublesome in terms of melting and “smearing” across the layers; in this result, however, there is no such problem evident.

### **3. Summary and Conclusion**

Foldable and rollable devices and displays present new challenges for both materials and processing technology, particularly when it comes to manufacturing a durable protective cover window. In this work, we investigated a high power picosecond UV laser for cutting a new material stack for this application, comprised of clear polyimide, durable hard coat, and a protective PET film. The ablation thresholds were successfully characterized for each of these layers and were found to vary by nearly a factor of ten. Based on these thresholds as well as other ablation behavior, layer-specific cutting processes were successfully developed, resulting in a high speed, high quality process for cutting the entire stack. HAZ extent was found to be well below 10  $\mu\text{m}$  for the most critical layers and the overall cutting speed achieved was  $>400$  mm/s. Hence, with careful process optimization of layer-specific parameter sets, picosecond UV lasers can successfully meet manufacturers needs for cutting these materials, helping to enable the proliferation of new, compact, and high-value foldable mobile devices into the marketplace.

### **References**

Liu, J.M., 1981. Simple Technique for Measurement of Pulsed Gaussian-Beam Spot Sizes, *Optics Letters*, Vol. 7, No. 5, p. 196.